# Level Structure of Low-Lying Excited States of $Sc^{46}$†

H. H. Bolotin
*Argonne National Laboratory, Argonne, Illinois*
(Received 16 November 1967)

The low-lying excited states of $Sc^{46}$ populated by primary and secondary $\gamma$-ray transitions from the $Sc^{45}(n,\gamma)Sc^{46}$ thermal-neutron-capture reaction were studied. Ge(Li) detectors were used exclusively in both singles and coincidence $\gamma$-ray investigations. High-energy primary $\gamma$-ray spectra were obtained and were used to infer the excitation energies of 53 states up to $\sim$2600 keV. The neutron binding energy was determined to be 8767±1 keV. Coincidence investigations between high-energy ($\sim$7–9 MeV) and low-energy ($\lesssim$2 MeV) $\gamma$ rays, as well as among the low-energy transitions, have allowed a total of 23 low-energy transitions to be assigned between states up to an excitation energy of 1324 keV. A level and decay scheme is proposed for a total of 57 excited states below an energy of 2600 keV. This scheme differs in several important respects from those proposed previously. The observed characteristics of these states are compared with the most recent charged-particle reaction studies, previous bent-crystal-spectrometer $\gamma$-ray results, and available theoretical calculations.

## I. INTRODUCTION

THE low-lying excited states of the odd-odd $Sc^{46}$ nuclide have been the subject of several intensive investigations[1–11] over the last few years. Only recently have improved experimental techniques[1–3] established the excitation energies of a number of these states up to an excitation energy of $\sim$1 MeV. The $(d,p)$ work of Rapaport *et al.*[1] has resulted in assignments of the orbital angular momentum of several of these states, and the bent-crystal-spectrometer studies of Van Assche *et al.*,[2] coupled with some of the scintillation coincidence data of Bolotin,[3] have led to a proposed level scheme[2] and the $\gamma$-ray branching of many of the low-lying states of $Sc^{46}$.

Although it is expected that the $(f_{7/2})^n$ shell-model configuration should play a dominant role in the make-up of the low-lying levels of $Sc^{46}$, considerations based upon the systematics of neighboring nuclides, and previously reported experimental investigations of the levels close to the $Sc^{46}$ ground state, lead to the conclusion that participation of other shell-model configurations must be included in any meaningful interpretation of the low-lying states of this nuclide. McCullen *et al.*[12] have presented the most definitive calculations on the low-lying $Sc^{46}$ states derived from the $(f_{7/2})^n$ configuration. Lawson *et al.*[13] have successfully accounted for the large retardations observed[14] for individual $M2$ transitions which proceed from $d_{3/2}$ proton-hole states in $Sc^{45}$ and $Sc^{47}$. In addition, $s_{1/2}$ proton-hole configurations might be expected to influence, to some extent, the constitution of states even below an excitation energy of 1500 keV in $Sc^{46}$. Thus, it is anticipated that there may be some fair degree of complexity in the shell-model characterization of the levels in $Sc^{46}$. It was felt that a comprehensive and careful reexamination of the levels of this nuclide by means of more advance experimental methods might realize additional and/or more detailed information concerning these levels and their $\gamma$-ray branching and that such results could be of effective aid in the interpretation of these low-lying states.

By virtue of the multiplicity of cascade $\gamma$ rays from the compound-nucleus state formed in thermal-neutron capture to low-lying levels of the product nucleus, states whose spins and parities may be significantly different from that of the initial capture state may readily be populated. Indeed, because of the statistical nature of

† Work performed under the auspices of the U. S. Atomic Energy Commission.

[1] J. Rapaport, A. Sperduto, and W. W. Buechner, Phys. Rev. **151**, 939 (1966).

[2] P. Van Assche, U. Gruber, B. P. Maier, H. R. Koch, and O. W. B. Schult, Nucl. Phys. **84**, 661 (1966).

[3] H. H. Bolotin, Phys. Rev. **138**, B795 (1965). To date, this work on the thermal-neutron-capture $\gamma$-ray reaction $Sc^{45}(n,\gamma)Sc^{46}$ was the most complete one that involved coincidence $\gamma$-ray spectroscopy. Unfortunately, at the time this work was reported, scintillation spectroscopy was the best means available for employment in these studies. Several important aspects of this work are confirmed in the present paper. Unhappily, the scintillation technique is hampered by poor energy resolution, and certain levels and cascade sequences reported in this work are not corroborated in either the present investigation or the bent-crystal-spectrometer work of Van Assche *et al.* (Ref. 2). However, several coincidence relationships established in this earlier work were utilized by the workers of Ref. 2 in the constructuion of their proposed level scheme.

[4] J. L. Yntema and G. R. Satchler, Phys. Rev. **134**, B976 (1964); J. L. Yntema and J. R. Erskine, Phys. Letters **12**, 26 (1964).

[5] E. der Mateosian and M. Goldhaber, Phys. Rev. **82**, 115 (1951); M. Goldhaber and C. O. Muehlhause, *ibid.* **74**, 1887 (1948).

[6] A. Andreeff, R. Kastner, and P. Manfrass, in *International Conference on the Study of Nuclear Structure with Neutrons, Antwerp, 1965* (North-Holland Publishing Co., Amsterdam, 1966).

[7] G. A. Bartholomew and B. B. Kinsey, Phys. Rev. **89**, 386 (1953); L. V. Groshev, V. N. Lutsenko, A. M. Demidov, and V. I. Pelekhov, *Atlas of γ-ray Spectra From Radiative Capture of Thermal Neutrons*, translated by J. B. Sykes (Pergamon Press, Ltd., London, 1959), p. 61.

[8] O. A. Wasson, Yale University Report No. 2627E-25, 1965 (unpublished).

[9] V. J. Orphan and N. C. Rasmussen, MIT Report No. MITNE-80, 1967 (unpublished).

[10] B. Hammermesh and V. Hummel, Phys. Rev. **88**, 916 (1952).

[11] J. M. Neill, N. C. Rasmussen, and T. J. Thompson, MIT Report No. MITNE-37, 1963 (unpublished).

[12] J. D. McCullen, B. F. Bayman, and L. Zamick, Phys. Rev. **134**, B515 (1964).

[13] R. D. Lawson, M. H. MacFarlane, M. Soga, and S. Cohen, Bull. Am. Phys. Soc. **9**, 650 (1964); R. D. Lawson and M. H. MacFarlane, Phys. Rev. Letters **14**, 152 (1965).

[14] R. E. Holland, F. J. Lynch, and K. E. Nystèn, Phys. Rev. Letters **13**, 241 (1964).

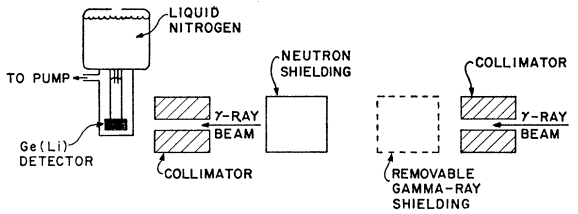


FIG. 1. Schematic representation of the tangential through-hole collimator system and Ge(Li) detector.

the wave function of the compound-nucleus state formed by neutron capture, $\gamma$-ray transitions proceeding either directly or by cascade to lower levels can populate such states to a degree that is in effect independent of their constitution. The combination of primary and secondary $\gamma$-ray transitions following thermal-neutron capture can equally well populate low-lying excited states characterized by excited neutron or proton configurations, by particle or hole makeup, or by an intrinsic, rotational, or vibrational nature. Thus, the neutron-capture process holds out the prospect of revealing levels that (a) are populated in charged-particle reactions, and/or (b) are *not* seen in these reactions because they are inhibited by considerations of angular momenta, particle or hole characteristics, etc. As a consequence of the foregoing, effectively all low-lying states are expected to be populated by the $(n,\gamma)$ reaction; and the use of sufficiently sophisticated experimental techniques to investigate this reaction can provide a valuable complement and extension to the information obtained from studies with $(d,p)$, $(d,t)$ and other reactions.

To this end, the present paper describes the results of an investigation of the low-lying excited states that are populated in the thermal-neutron capture reaction $Sc^{45}(n,\gamma)Sc^{46}$, and of the transitions among them. These studies were conducted by means of singles and coincidence $\gamma$-ray techniques which made exclusive use of Ge(Li) solid-state detectors. These studies involved coincidence data recorded between the high-energy ($\sim$8 MeV) primary transitions and the subsequently-emitted low-energy transitions, as well as coincidences among the low-energy cascade $\gamma$ rays.

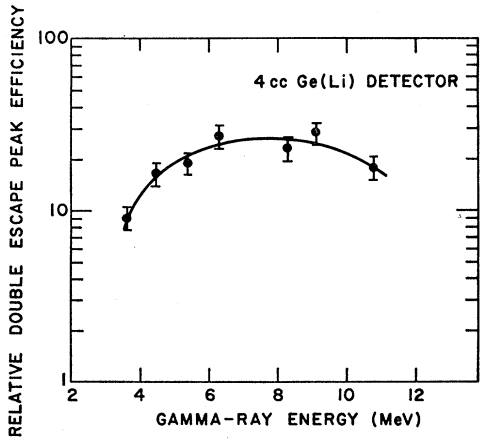


FIG. 2. Empirically determined relative double-escape-peak efficiency of the Ge(Li) detector system as a function of $\gamma$-ray energy.

## II. EXPERIMENTAL FACILITIES AND TECHNIQUES

### A. High-Energy Singles $\gamma$-Ray Facility

A target of high-purity $Sc_2O_3$ was installed at the center of the tangential through-tube facility at the Argonne CP-5 reactor. The thermal-neutron flux at this position was $\sim 3\times 10^{13}$ neutrons $cm^{-2}$ $sec^{-1}$. This facility, which is described in detail elsewhere,[15] allows a highly collimated beam of the high-energy capture $\gamma$ rays emitted by the target to emerge from the reactor tube and to be incident upon a well-shielded Ge(Li) detector. A schematic representation of the beam collimator and Ge(Li) detector system is shown in Fig. 1. The Ge(Li) detector had a sensitive volume of $\sim$4 $cm^3$ and an energy resolution width of $\sim$6 keV at a deposited energy of 6 MeV. Figure 2 displays the relative efficiency for detection of the double-escape peak as a function of $\gamma$-ray energy for the detector-collimator system. This curve was empirically determined by comparing the peak intensities observed from a nitrogen sample with the known[16] relative intensities of the transitions.

In order to reduce background contamination, the angle of view of the collimator was restricted to include only the area occupied by the sample; $\gamma$ rays originating from the liner of the through tube were screened off. Nitrogen contamination was purged by flowing He gas through the reactor tube. The use of high-purity graphite sample holders afforded the combined advantages of low capture cross section and a spectrum in which the only contaminant peaks were from the two high-energy $\gamma$-ray transitions at 4945 and 3684 keV, which arise from capture in the holder. In addition, these two $\gamma$ rays, whose energies have been determined to high precision,[17] served as convenient $\gamma$-ray energy standards. Other sources of background were materially reduced by appropriate shielding.

This facility was used to view the high-energy primary $\gamma$-ray transitions. Low-energy transitions were so strongly attenuated in the neutron shielding material placed between the reactor orifice and the Ge(Li) detector that they could not be utilized to any meaningful extent.

The entire spectrum was recorded in 4096-channel pulse-height analyzer for which no electronic biasing arrangement was employed. Digital zero and gain stabilization was employed at the ADC of the analyzer to

[15] G. E. Thomas, D. E. Blatchley, and L. M. Bollinger, Nucl. Instr. Methods (to be published).
[16] H. T. Motz, R. E. Carter, and W. D. Barfield, *Pile Neutron Research in Physics* (International Atomic Energy Agency, Vienna, 1962).
[17] W. V. Prestwich (private communication).

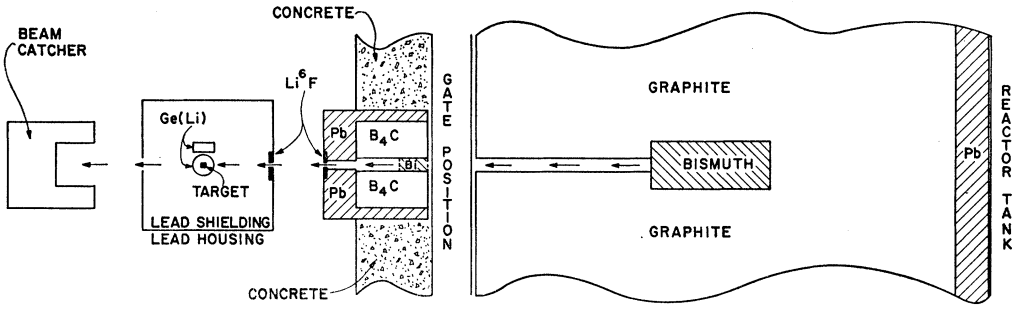


FIG. 3. Representation of the external thermal-neutron beam facility.

avoid the usual difficulties associated with electronic drifts to which the high-energy pulse-height region is extremely sensitive. No gain shift or line broadening was evident in runs lasting in excess of 24 h. In order to accurately determine the energies of the spectral lines, the system was periodically calibrated with a voltage pulser. The centroids of both spectrum lines and calibration lines and the peak areas of the $Sc^{46}$ lines were determined by a computer program[18] which employed a Gaussian line shape in a variable-metric minimization procedure. In conjunction with this calibration method, the carbon ground-state $\gamma$ ray (4945.4 keV)[17] and the 0.511-MeV annihilation radiation peaks in the spectrum were employed as energy standards. This analysis permitted the determination of the $\gamma$-ray energies of the stronger and/or more isolated $Sc^{46}$ peaks within an uncertainty of $\sim$1 keV.

This analysis took account of the presence of double- and single-escape peaks, as well as of the full-energy peaks which were observed for the stronger transitions. The ratio of the detection efficiency for the double-escape peak to that for single escape was found to be 10:1, independent of energy. The efficiency for double-escape peaks was observed to be $\sim$10 times that for full-energy peaks at $E_\gamma=4$ MeV, and this ratio increased monotonically to $\sim$30 at $E_\gamma=9$ MeV. Some spectral regions were complicated by the close proximity of the various types of lines associated with different $\gamma$ rays. To clarify these situations and to corroborate the identification of certain lines as double-escape peaks, the detector system was operated in a pair-spectrometer mode in which the Ge(Li) detector was straddled by two 4×4-in. NaI(Tl) scintillators mounted 180° apart. The relatively small solid angle of this pair-spectrometer arrangement reduced the counting rate in the double-escape peak to about 5% of that for the singles mode of operation. Hence, the pair mode was utilized mainly for clarification and confirmation; the singles spectrum was used for the main analysis.

[18] W. C. Davidon, Argonne National Laboratory Report No. ANL-5990 (Rev. 2), 1966 (unpublished); H. H. Bolotin, in *Slow-Neutron Capture Gamma-Ray Spectroscopy*, edited by H. H. Bolotin, Argonne National Laboratory Report No. ANL-7282, 1966, paper D-3 (unpublished).

### B. External-Beam Facility

An external-beam facility was empolyed to carry out low-energy singles and coincidence $\gamma$-ray investigations of high- and low-energy and of low- and low-energy $\gamma$-ray cascades. These studies were made with the exclusive use of Ge(Li) detectors[19] in order to obtain experimental data with the highest possible energy resolution. A highly collimated external beam of thermal neutrons, effectively free of fast neutrons (Cd ratio$\approx$550) and pile $\gamma$ rays, was extracted from a modified thermal-column facility at the Argonne CP-5 reactor. A schematic representation of this facility is shown in Fig. 3. An extremely well-defined thermal-neutron beam (thermal flux$\approx 5\times10^7$ neutrons $cm^{-2}$ $sec^{-1}$, diameter$\approx$0.75 in.) was obtained by means of a conventional collimator fitted with defining apertures of $Li^6F$ disks enriched[20] to 95.5% in $Li^6$. The targets consisted of pressed cylindrical pellets of high-purity $Sc_2O_3$ which were contained in thin (4.5 mg/$cm^2$) aluminum holders.

Two planar drifted Ge(Li) detectors (each$\sim$3.5 $cm^3$ active volume) were mounted at right angles to each other and positioned 1.5 in. from the beam axis. Both detectors were shielded by thin (0.25-cm thick)$Li^6F$ disks to prevent scattered neutrons from entering the detectors or detector housings.

The $\gamma$-$\gamma$ coincidence data were stored on a two-parameter magnetic-tape storage unit in a 1024×1024-channel pulse-height array. A 4096-channel ADC was empolyed in each leg of the coincidence system in order to obtain the pulse-height resolution capabilities of the large ADC's while any desired 1024-channel segment of each 4096-channel spectrum was selected for storage. The storage capacity of the magnetic tape was $\sim 2.75\times10^6$ event-address pairs.

A time-to-pulse-height converter[21] served as the basis of the fast coincidence timing unit. The output signals of two highly stable single-channel pulse-height anal-

[19] A preliminary description of the use of this method in thermal-neutron-capture $\gamma$-ray studies was included in a paper presented by the author at the Conference on Semiconductor Nuclear Radiation Detectors and Circuits, Gatlinburg, Tenn., 1967 (unpublished).

[20] Fabricated by Oak Ridge Stable Isotopes Sales, Oak Ridge National Laboratory, Oak Ridge, Tenn.

[21] R. Roddick and F. J. Lynch, IEEE Trans. Nucl. Sci. **11**, 399 (1964).

TABLE I. Summary of the primary high-energy $\gamma$-ray energies and relative intensities, and the excitation energies of states populated directly from the capture state of the thermal-neutron-capture reaction $Sc^{45}(n,\gamma)Sc^{46}$.

| Transition number | Excitation energy[a] (keV) | $\gamma$-ray energy (keV) | Relative intensity[b] |
|---|---|---|---|
| 1 | 0 | 8767±1 | 7.4±1.1 |
| 2 | 142 | 8624±1 | 2.2±0.3 |
| 3 | 227 | 8539±1 | 45 ±7 |
| 4 | 289 | 8477±1 | 6.9±1.0 |
| 5 | 444 | 8321±1 | 20 ±3 |
| 6 | 585 | 8182±1 | 100 |
| 7 | 627 | 8139±1 | 27 ±4 |
| 8 | 835 | 7930±1 | 5.9±0.9 |
| 9 | 1089 | 7675±1 | 4.0±0.6 |
| 10 | 1125 | 7641±1 | 28 ±4 |
| 11 | 1133 | 7633±3 | 2.3±0.4 |
| 12 | 1273 | 7494±1 | 5.7±0.9 |
| 13 | 1324 | 7442±1 | 2.5±0.4 |
| 14 | 1391 | 7375±2 | 0.5±0.2 |
| 15 | 1397 | 7370±2 | 1.2±0.2 |
| 16 | 1422 | 7345±3 | 0.5±0.3 |
| 17 | 1430 | 7336±2 | 3.7±0.6 |
| 18 | 1529 | 7238±2 | 8.0±1.3 |
| 19 | 1645 | 7121±1 | 32 ±5 |
| 20 | 1711 | 7055±1 | 5.7±0.9 |
| 21 | 1766 | 7001±2 | 2.7±0.5 |
| 22 | 1803 | 6964±1 | 3.7±0.6 |
| 23 | 1837 | 6930±3 | 0.9±0.2 |
| 24 | 1890 | 6876±2 | 13.5±2.1 |
| 25 | 1914 | 6852±4 | 3.2±0.8 |
| 26 | 1924 | 6842±1 | 92 ±14 |
| 27 | 1934 | 6833±3 | 2.1±1.0 |
| 28 | 2046 | 6720±1 | 29 ±4 |
| 29 | 2074 | 6693±4 | 3.1±0.7 |
| 30 | 2089 | 6678±4 | 2.0±0.9 |
| 31 | 2117 | 6650±2 | 9.9±1.6 |
| 32 | 2122 | 6644±2 | 11.5±2.0 |
| 33 | 2131 | 6635±2 | 1.1±0.3 |
| 34 | 2156 | 6610±3 | 0.8±0.4 |
| 35 | 2207 | 6560±1 | 44 ±7 |
| 36 | 2225 | 6542±2 | 4.4±0.7 |
| 37 | 2257 | 6509±2 | 9.2±1.4 |
| 38 | 2297 | 6470±3 | 2.3±0.4 |
| 39 | 2306 | 6460±1 | 11.8±1.8 |
| 40 | 2333 | 6433±1 | 1.6±0.3 |
| 41 | 2401 | 6366±3 | 13.4±2.2 |
| 42 | 2415 | 6352±1 | 54 ±8 |
| 43 | 2436 | 6330±4 | 3.0±0.6 |
| 44 | 2446 | 6320±1 | 61 ±9 |
| 45 | 2455 | 6312±3 | 8.9±1.4 |
| 46 | 2463 | 6303±2 | 18 ±3 |
| 47 | 2525 | 6242±5 | 2.2±0.7 |
| 48 | 2532 | 6234±5 | 1.2±0.6 |
| 49 | 2544 | 6223±5 | 2.0±0.6 |
| 50 | 2554 | 6212±5 | 3.3±0.8 |
| 51 | 2561 | 6205±4 | 8.9±1.4 |
| 52 | 2572 | 6195±2 | 12.5±2.0 |
| 53 | 2582 | 6184±5 | 3.7±0.8 |
| 54 | 2593 | 6173±1 | 51 ±8 |
| 55 | ··· | 6119±2 | 4.7±0.8 |
| 56 | ··· | 6100±2 | 9.5±1.5 |
| 57 | ··· | 6068±2 | 8.3±1.3 |
| 58 | ··· | 6057±1 | 32 ±5 |
| 59 | ··· | 6048±1 | 14.7±2.2 |
| 60 | ··· | 5980±1 | 7.0±1.0 |
| 61 | ··· | 5928±4 | 3.3±0.8 |
| 62 | ··· | 5907±3 | 13.4±2.2 |
| 63 | ··· | 5899±1 | 49 ±8 |
| 64 | ··· | 5874±4 | 2.6±0.5 |
| 65 | ··· | 5868±5 | 2.5±0.6 |
| 66 | ··· | 5860±3 | 1.6±0.3 |
| 67 | ··· | 5822±2 | 4.7±0.8 |
| 68 | ··· | 5804±2 | 5.5±0.9 |
| 69 | ··· | 5795±3 | 3.5±0.6 |
| 70 | ··· | 5783±2 | 10.0±1.5 |
| 71 | ··· | 5759±5 | 1.9±0.5 |
| 72 | ··· | 5745±1 | 25 ±4 |
| 73 | ··· | 5730±4 | 5.2±1.2 |
| 74 | ··· | 5721±3 | 5.8±0.9 |
| 75 | ··· | 5705±2 | 4.6±0.8 |
| 76 | ··· | 5680±3 | 7.9±1.3 |
| 77 | ··· | 5667±2 | 19 ±3 |
| 78 | ··· | 5651±5 | 2.4±0.5 |
| 79 | ··· | 5638±5 | 1.3±0.3 |
| 80 | ··· | 5624±2 | 25 ±3 |
| 81 | ··· | 5595±5 | 1.2±0.3 |
| 82 | ··· | 5584±2 | 16.8±2.7 |
| 83 | ··· | 5568±3 | 9.3±1.5 |
| 84 | ··· | 5557±4 | 9.8±1.7 |
| 85 | ··· | 5539±4 | 1.3±0.6 |
| 86 | ··· | 5532±2 | 12.1±2.0 |
| 87 | ··· | 5521±5 | 1.5±0.4 |
| 88 | ··· | 5502±2 | 7.9±1.2 |
| 89 | ··· | 5484±2 | 22.5±3.5 |
| 90 | ··· | 5455±4 | 10.1±1.9 |
| 91 | ··· | 5447±3 | 22.2±3.7 |
| 92 | ··· | 5418±4 | 1.4±0.3 |
| 93 | ··· | 5400±5 | 1.4±0.3 |
| 94 | ··· | 5380±2 | 10.8±1.7 |
| 95 | ··· | 5365±2 | 10.6±1.7 |
| 96 | ··· | 5348±2 | 14.3±2.2 |
| 97 | ··· | 5337±2 | 28 ±4 |
| 98 | ··· | 5318±2 | 8.4±1.4 |
| 99 | ··· | 5297±5 | 2.9±0.7 |
| 100 | ··· | 5287±2 | 19 ±3 |
| 101 | ··· | 5268±2 | 54 ±9 |
| 102 | ··· | 5227±5 | 6.1±2.0 |
| 103 | ··· | 5219±5 | 2.5±0.7 |
| 104 | ··· | 5211±2 | 16.7±2.8 |
| 105 | ··· | 5164±1 | 21.4±3.5 |
| 106 | ··· | 5155±2 | 8.6±1.4 |
| 107 | ··· | 5140±5 | 6.5±1.2 |
| 108 | ··· | 5129±3 | 13.1±2.2 |
| 109 | ··· | 5106±5 | 6.8±1.9 |
| 110 | ··· | 5085±2 | 18.6±3.0 |
| 111 | ··· | 5053±3 | 7.4±1.4 |
| 112 | ··· | 5039±4 | 6.1±1.1 |
| 113 | ··· | 4994±1 | 29.3±4.3 |
| 114 | ··· | 4975±1 | 75 ±11 |
| 115 | ··· | 4919±2 | 13.8±2.2 |
| 116 | ··· | 4899±5 | 1.7±0.6 |
| 117 | ··· | 4891±2 | 17.8±2.8 |
| 118 | ··· | 4883±2 | 18.5±2.9 |
| 119 | ··· | 4875±4 | 2.5±0.6 |
| 120 | ··· | 4822±2 | 14.4±2.4 |
| 121 | ··· | 4812±5 | 5.6±1.1 |
| 122 | ··· | 4775±5 | 1.4±0.5 |

[a] All of the listed excitation energies were determined from the measured neutron binding energy and the energies of those transitions which were taken as primary $\gamma$ rays under the usual and reliable assumption that (except for the group of very light nuclides) transitions that have energies $\gtrsim 70\%$ of the binding energy are primary. A considerable number of transitions with energies lower than this conservative criterion were observed. Many of these transitions are most probably primary, and if so taken agree quite well with transitions terminating at states observed in previously reported $(d,p)$ work (Ref. 1). However, since these transition energies do not meet the criterion adopted for their assignment as primary $\gamma$ rays, the excitation energies of the terminal states of these transitions have been omitted. It works little hardship on the reader to supply these excitation energies from the listed transition energies numbered 55–122 if subsequent findings offer stronger evidence that they are primary.

[b] The errors assigned to the relative intensities listed here also reflect the ~15% uncertainty quoted for the intensities of the transitions in nitrogen (Ref. 16) which were used in the empirical determination of the relative double-escape-peak detection efficiencies of the Ge(Li) detector (Fig. 2). The strengths of all lines listed have been corrected for detector efficiency and have been normalized to that of the strongest transition (8182 keV) observed in the spectrum. No attempt was made to establish the intensities of these transitions in percent per neutron capture by comparing the relative intensities observed with those of Ref. 7. The spectra observed by these authors contain too large a number of unresolved transitions for such a comparison to be feasible.

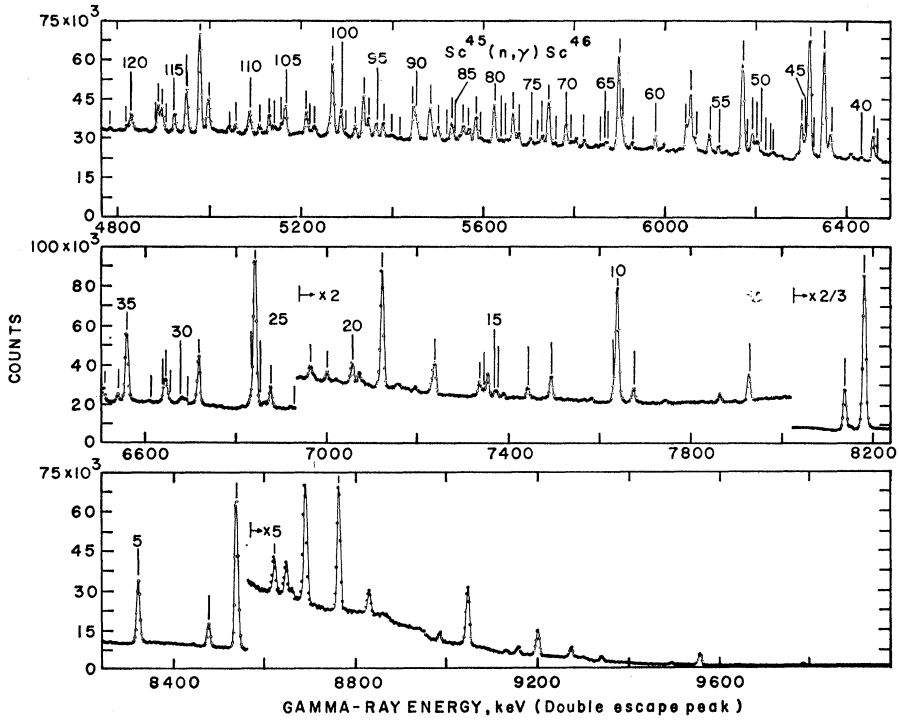


FIG. 4. Typical high-energy Ge(Li) singles pulse-height spectrum obtained for the reaction $Sc^{45}(n,\gamma)Sc^{46}$. The abscissa denotes the $\gamma$-ray energy to be associated with the double-escape peaks in the spectrum. The double-escape peaks are numbered to correspond to those $\gamma$-rays listed in Table I.

yzers—one set of the prompt time pulse-height distribution and the other set of the chance portion of the distribution—were recorded on the magnetic tape as fast-coincidence "total" and "chance" labels for each recorded event which satisfied the triple slow-coincidence requirement. Thus, the total and chance coincidence spectra were simultaneously registered and were separately scanned during the tape-searching process with the aid of these assignation labels.

Two separate sets of $\gamma$-$\gamma$ coincidence studies were conducted. One detector was always set to record the low-energy portion of the spectrum while the second detector registered either (a) the high-energy spectrum ($\sim$7–9 MeV) or (b) the low-energy spectrum.

The energy resolution of the Ge(Li) detector is sufficient to delineate single primary transitions which signal the population of individual low-lying states. Coincidence spectra recorded between these $\gamma$-ray transitions and the low-energy transitions issuing and cascading from these particular states are capable of defining both the decay characteristics of these states and the subsequent population and decay of lower levels. The coincidence relationships established among the group of low-energy transitions serve to complement and extend the information gleaned from the high-energy/low-energy coincidence studies.

## III. RESULTS

### A. High-Energy Spectrum

Figure 4 displays the singles spectrum of the primary high-energy capture $\gamma$ rays from the reaction $Sc^{45}(n,\gamma)Sc^{46}$. This spectrum was recorded in a run lasting 24 h. The analysis based on this spectrum yielded assignments of double-escape, single-escape, and full-energy peaks that are felt to be unambiguous. Without exception, these double-escape peak assignments were corroborated by the pair-spectrometer spectrum (which records only double-escape peaks) taken over the identical energy range. The high-energy $\gamma$-ray energies and relative intensities determined for this reaction are listed in Table I. The excitation energies of terminal states so populated have been obtained under the usual and well-founded assumption that, in this mass region, $\gamma$ rays that have energies $\gtrsim 70\%$ of the neutron binding energy are primary transitions proceeding directly from the capture state to low-lying excited states.

The neutron binding energy was determined to be $8767\pm1$ keV from the energy of the observed primary transition to the ground state. (This ground-state assignment is confirmed in Sec. IIIB.) This value of the neutron separation energy is in excellent agreement with the value $8766\pm5$ keV reported by Wasson[8] from an investigation of the same reaction, the mass-adjusted value[22] of $8767\pm4$ keV and the neutron binding energy of $8764\pm8$ keV derived from the $(d,p)$ $Q$ value reported by Rapaport *et al.*,[1] but deviates slightly from the value $8760.5\pm1.0$ keV derived from the $(n,\gamma)$ studies of Orphan *et al.*[9] Spectral complexities and other sources of uncertainties combined to terminate efforts for further analysis below a $\gamma$-ray energy of $\sim$4800 keV.

[22] J. H. E. Mattauch, W. Thiele, and A. H. Wapstra, Nucl. Phys. **67**, 32 (1965).

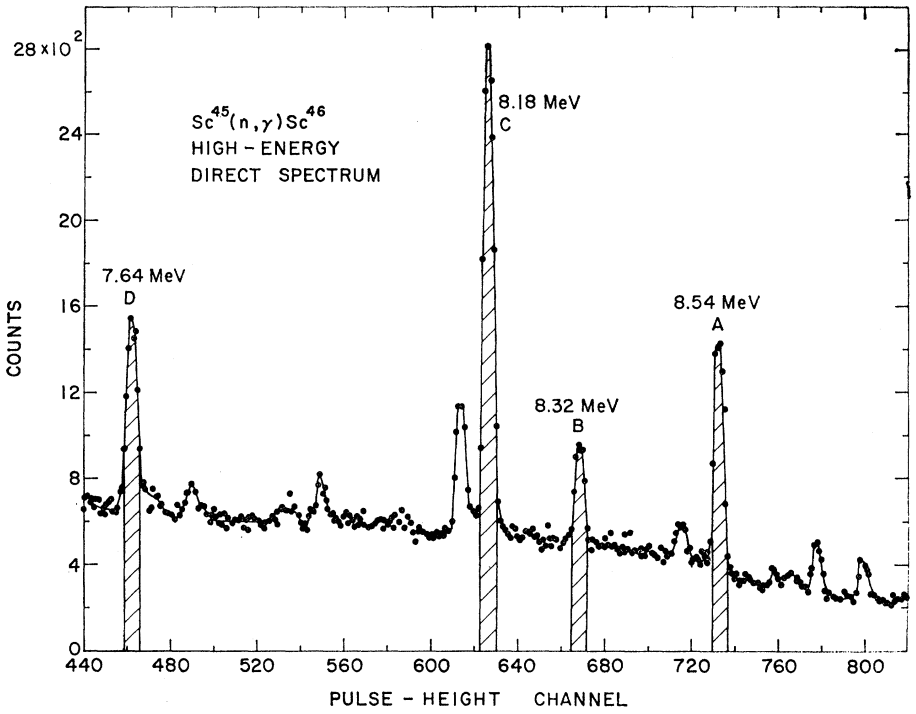


FIG. 5. Representative high-energy Ge(Li) singles pulse-height spectrum obtained in the external beam arrangement for the reaction $Sc^{45}(n,\gamma)Sc^{46}$. The lettered and cross-hatched double-escape peaks are the ones that served as coincidence gates in the two-parameter magnetic-tape-searching procedure for the low-energy coincidence spectra shown in Fig. 6. The double-escape peaks are labeled with their respective $\gamma$-ray energies.

The summary of high-energy $\gamma$ rays presented in Table I contains 122 transitions down to a $\gamma$-ray energy of 4775 keV. The excitation energies of the terminal levels of the 54 highest energy $\gamma$ rays that satisfied the criterion adopted for the assignment of primary transitions are also specified in Table I. It should be pointed out that there is a considerable numer of the lower energy transitions which, if considered primary, lead to population of states whose excitation energies are in good agreement with some of the states observed in the $(d,p)$ work of Rapaport *et al.*[1] However, since the energies of these $\gamma$ rays do not fully meet the self-imposed (albeit conservative) definition of "primary," and since there could well be accidental agreement between the energies that would correspond to the terminal states of these $\gamma$ rays and the energies of the $(d,p)$-excited states, the other 68 transitions of lower energy have been arbitrarily excluded from the primary category. The energies of these transitions are listed in Table I so that the associated excitation energies of their terminal states can be specified if further evidence leads to their assignment as primary $\gamma$ rays.

### B. Low-Energy Transitions and $\gamma$-$\gamma$ Coincidence Studies

#### 1. *Low-Energy $\gamma$-Ray Singles Measurements*

The spectrum of low-energy $\gamma$ rays from the $Sc^{45}(n,\gamma)Sc^{46}$ reaction was recorded in the external-beam facility. The energy calibration was obtained by use of well-known energy standards and a series of pulser calibration peaks in a manner analogous to that utilized for the primary $\gamma$-ray spectrum. In the energy range below $\sim$2 MeV, the detection efficiency of the Ge(Li) detector employed was determined for each peak with the aid of single $\gamma$-ray lines from intensity-calibrated sources.[23] Table II lists the energies and relative intensities of the transitions observed up to an energy of $\sim$900 keV. These entries are generally in good agreement with those of Van Assche *et al.*[2] and Orphan *et al.*[9]

#### 2. *High-Low $\gamma$-$\gamma$ Coincidences*

Two-parameter $\gamma$-$\gamma$ coincidence spectra were recorded with one Ge(Li) detector set to accept the high-energy primary transitions in the $\gamma$-ray energy range from $\sim$6.8–9 MeV, while the second Ge(Li) detector viewed the low-energy events up to a $\gamma$-ray energy of $\sim$2 MeV. These coincidence spectra were recorded over a 100-h period. A portion of a singles high-energy spectrum, delineating particular primary transitions that served as coincidence gates, is shown in Fig. 5. Representative portions of the spectra of low-energy events in coincidence with these high-energy pulse-height gates are displayed in Fig. 6. No statistically meaningful coincidence peaks were observed in the energy range between $\sim$900 and 2000 keV.

In addition to other pertinent information, these data provide unambiguous corroboration that the terminal state of the 8767-keV transition, whose energy was adopted as the neutron binding energy, is indeed the ground state. The $\gamma$-ray coincidence relationships, as

[23] Obtained from D. W. Engelkemeir.

determined from this series of spectra, are summarized in Table III.

The $\gamma$-ray decays of those low-lying states directly populated by the selected primary transitions are seen to be distinctive, and relatively free of complexity. It is evident that had a NaI(Tl) detector been empolyed to view the high-energy transitions, the lack of good energy resolution would have prevented the clear-cut selection of individual transitions. Even if Ge(Li) detectors had been used to register these transitions, but NaI(Tl) scintillators had been used for the low-energy $\gamma$ rays, the important separation of closely spaced transitions (such as the 216- and 227-keV peaks) would not have been possible. Thus, in order to fully exploit the coincidence technique and to obtain meaningful and unequivocally definitive spectra, is was necessary to employ Ge(Li) in both arms of the coincidence system. The detection efficiency of such a combination of solid-state detectors is considerably lower than that of a NaI(Tl)-Ge(Li) detector pair, but the increased clarity and unambiguous quality of the resultant spectra obtained with two Ge(Li) detectors more than compensates for the efficiency loss. Indeed, it is required in order to clearly establish the coincidence relationships among the $\gamma$-ray transitions.

TABLE II. Summary of the energies and relative intensities of the low-energy $\gamma$ rays included in the proposed decay scheme of Fig. 9.

| Transition energy[a] (keV) | Relative $\gamma$-ray intensities[b] |
|---|---|
| 52.0 | 8.9 |
| 142.5 | 33 |
| 147.0 | 39 |
| 216.1 | 20 |
| 227.8[c] | 68[c] |
| 228.7[c] | 32[c] |
| 280.8 | 1.9 |
| 295.2 | 34 |
| 400.1 | 2.0 |
| 486.2 | 3.4 |
| 497.9 | 0.4 |
| 539.2 | 5.7 |
| 547.3 | 2.0 |
| 554.5 | 13.9 |
| 585.0 | 16.0 |
| 627.5 | 18.8 |
| 722.1 | 4.4 |
| 773.9 | 4.3 |
| 807.6 | 4.2 |
| 835.2 | 1.4 |
| 844.0 | 1.1 |
| 860.7 | 3.4 |
| 899.0 | 2.2 |

[a] The estimated errors assigned to the transition energies are ~0.4 keV for energies <300 keV and ~0.7 keV for those of higher energy.
[b] The relative intensities of the $\gamma$ rays were normalized to the sum of the intensities observed for the 227.8- and 228.7-KeV transitions which were unresolved in the present investigation. An ~15% error is to be associated with these values.
[c] Since these $\gamma$ rays were unresolved in the present work, the energies and relative intensities were taken from the work of Ref. 2. It should be pointed out that the average of their energies, weighted by their quoted intensities, differs by less than 0.1 keV from that determined for the unresolved doublet in the present investigation.

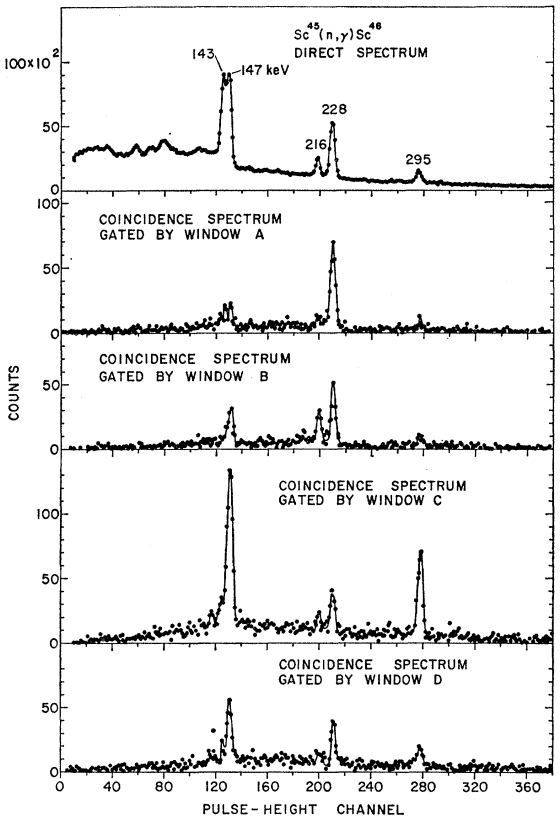


FIG. 6. Representative portions of the low-energy spectra in coincidence with the correspondingly labeled high-energy transitions shown in Fig. 5. The upper curve is the singles spectrum recorded under the same experimental conditions as the four lower coincidence spectra. In this figure, no corrections have been made for the presence of chance coincidences or of coincidences with transitions of higher pulse heights whose continua underlie the particular high-energy coincidence gates employed. The contribution from chance coincidences can be assessed by comparing the magnitude of the 142-keV transition (which follows the decay of the 142-keV 19-sec isomeric level and for which no prompt coincidences are recorded) in the coincidence spectra with that of the same transition in the singles spectrum (upper portion of figure) whose shape the chance coincidence spectrum follows.

### 3. *Low-Low $\gamma$-$\gamma$ Coincidences*

In this series of runs, both Ge(Li) detectors were set to view the low-energy $\gamma$-ray spectra below ~1600 keV. The acquisition of these data required an experimental running time of ~40 h. Representative portions of these low-low coincidence spectra are shown in Fig. 7. All low-low coincidence transitions that are considered well-defined are tabulated in Table IV.

The combination of increased detection efficiency and the higher intensity of the low-energy $\gamma$ rays resulted in coincidence spectra of good statistical quality. Again, had either arm of the coincidence system been a NaI(Tl) detector, the individual lines in regions of close-lying peaks could not have been selected unambiguously by the coincidence gate nor could these multiplets have been separated in the gated coincidence spectra. Thus even in the case of low-low coincidences, the use of two

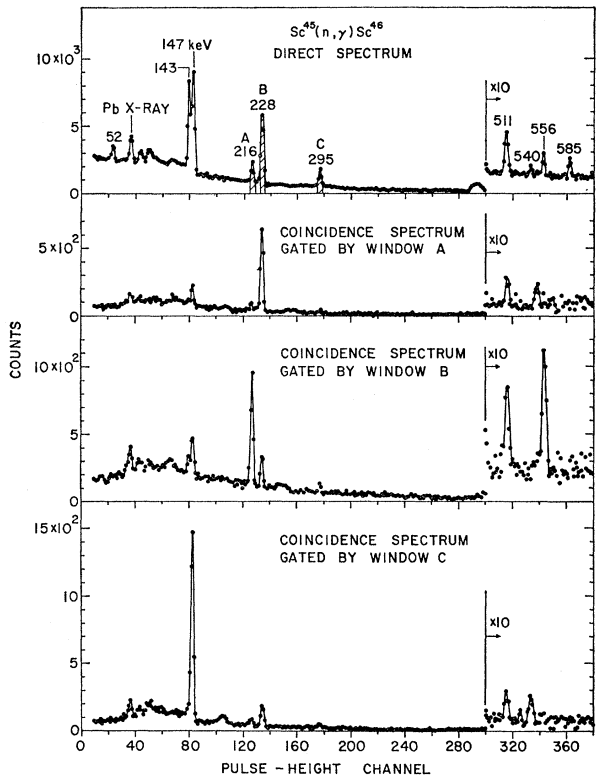


FIG. 7. Typical portions of the low-energy spectra in coincidence with the particular low-energy coincidence gates specified by the cross-hatched peaks of the singles spectrum shown in the upper portion of this figure. The three lower coincidence spectra shown have not been corrected for chance coincidences or for coincidence contributions due to those portions of the Compton distributions of higher energy transitions which underlie the respective coincidence gates used. The chance contribution can be estimated from a comparison of the singles spectrum (whose shape the chance coincidence spectrum follows) and the magnitude of the 142-keV peak (which follows the decay of the noncoincident 19-sec isomeric level) in the coincidence spectra.

Ge(Li) detectors is dictated by the experimental situation.

## IV. LEVEL SCHEME

The results of the primary high-energy singles $\gamma$-ray studies listed in Table I have established the positions of 53 excited states up to 2593 keV. In Fig. 8 the states below an excitation energy of $\sim$2600 keV in $Sc^{46}$, which previous workers[8,9] and the present author observed to be populated by primary transitions following the reaction $Sc^{45}(n,\gamma)Sc^{46}$, are compared schematically with those excited states reported by Rapaport *et al.*[1] in their $(d,p)$ studies. Every state that Wasson[8] observed to be fed by primary transitions has been corroborated in the present work. Conversely, the improved experimental conditions of the present work permitted the observation of a host of levels and/or the resolution of closely spaced doublets, etc., which were not defined in Wasson's study

TABLE III. Results of coincidence studies between high-energy primary and low-energy $\gamma$ rays.

| Energies of primary transitions (keV) | Energies of coincident low-energy $\gamma$ rays (keV) |
|---|---|
| 8539 | 227 |
| 8477 | 147 |
| 8321 | 216, 227 |
| 8182 | 147, 295, 585 |
| 8139 | 627 |
| 7930 | 228, 554 |
| 7641 | 147, 295, 539, 585 |

TABLE IV. Results of coincidence studies among the low-energy $\gamma$ rays.

| Energy of $\gamma$-ray transition (keV) | Energies of coincident $\gamma$ rays (keV) |
|---|---|
| 147 | 295, 539 |
| 216 | 227, 547 |
| 227 | 216, 547, 860 |
| 228 | 486, 554, 808 |
| 295 | 147, 539 |
| 539 | 147, 295, 585 |
| 554 | 228, 486 |
| 585 | 539 |

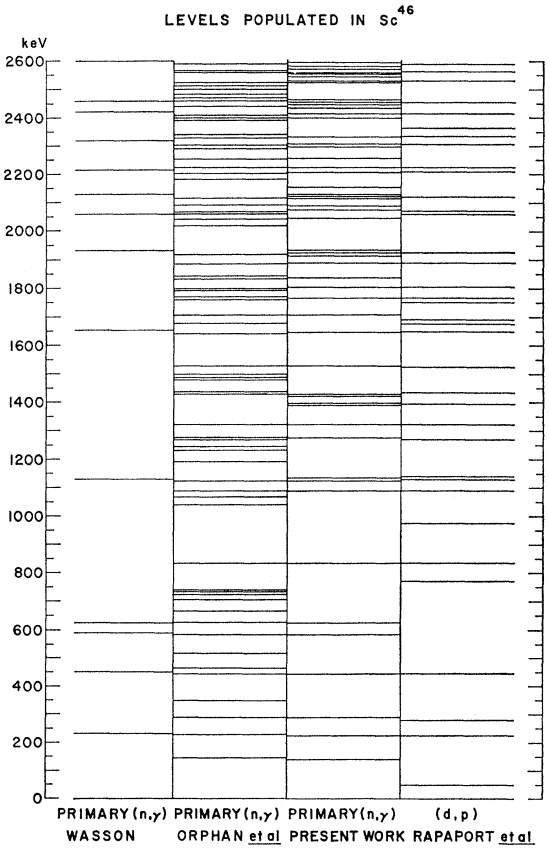


FIG. 8. Comparison of the states observed to be populated by primary transitions following the reaction $Sc^{45}(n,\gamma)Sc^{46}$ in the experiments reported in Refs. 8, 9, and the present work, together with those excited states seen in the $(d,p)$ studies of Ref. 1, up to an excitation energy of $\sim$2600 keV.

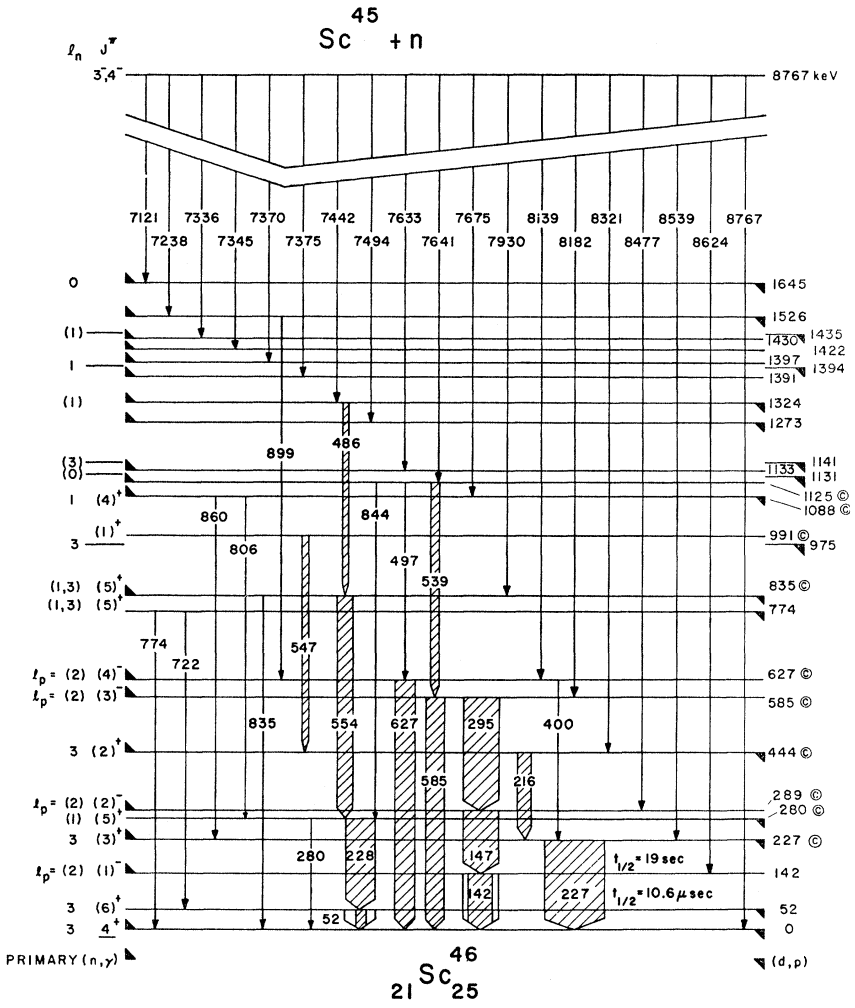


FIG. 9. Proposed level scheme of $Sc^{46}$ deduced from the various coincidence and singles $\gamma$-ray investigations of the present work. This scheme was constructed without recourse to either the previously reported $(n,\gamma)$ bent-crystal-spectrometer results (Ref. 2) or the $(d,p)$ work of Rapaport *et al.* (Ref. 1). The excitation energies are expressed in keV. Those levels marked on the left by upward-pointing flags are those that were observed to be populated by primary transitions from the capture state. Those levels marked on the right by downward-pointing flags are levels associated with reported $(d,p)$ population. The levels observed to be populated in the present work are designated by full horizontal lines across the level scheme. The $(d,p)$ states whose identification with the $(n,\gamma)$ levels is somewhat doubtful because their energies do not quite agree are shown as short lines at the right and again at the left, with no connection across the diagram. The states designated by © are those that were established in the present work on the basis of the presently reported coincidence studies. The 774-keV state is the only level presented which is based solely upon the energy balance of low-energy transitions. Consequently, it is not proposed as confidently as are the states assigned on the basis of the coincidence results. The proposed spins and parities of the levels are shown immediately to the left of the levels. The capture state is characterized by spin $3^-$ and/or $4^-$. The $l_n$ values reported in $(d,p)$ studies (Ref. 1) are shown at the extreme left. Those $l_n$ values that were deemed uncertain by the authors of the $(d,p)$ work, or that the present author judged to be equivocal on the basis of the angular distributions presented in Ref. 1, are enclosed in parentheses. The levels designated by $l_p=2$ are tentatively assigned from the $Ti^{47}(d,He^3)Sc^{46}$ work of Ref. 4.

of the same reaction. However, a comparison (Fig. 8) of the present work with that of Orphan *et al.*[9] reveals the somewhat larger number of transitions reported in their study of the primary transitions. Without exception, the relative intensities these authors ascribe to these additional transitions are small. Despite this, a few of these $\gamma$ rays have intensities[9] equal to, or somewhat greater than, those of transitions seen in the present investigation. It may be of interest to note that of their 19 additional transitions that correspond to terminal states below ~1500-keV excitation, not one feeds a level seen in the $(d,p)$ studies.[1] Although it is possible that all of these levels are too weakly populated in $(d,p)$ stripping to have been observed, the probability for this nonconcurrence is quite small—especially since the spectra of states populated both by primary $\gamma$ rays and by $(d,p)$ stripping show no evidence of correlation between the intensities of population by the two processes.

All of these additional lines are sufficiently displaced in energy from other transitions to remove the possibility of a masking effect due to close-lying transitions. It is therefore surprising that, with comparable energy

resolution in these two sets of investigations, neither in the presently reported high-energy singles spectrum (recorded with much better statistical accuracy than the spectrum obtained by the MIT group[9]) nor in the pair-spectrometer run of the present work (also obtained with higher statistical accuracy and with a larger peak-to-underlying-continuum ratio than the pair-spectrometer spectrum obtained by Orphan *et al.*[9]) was even the strongest of these additional transitions observed in the presently reported investigation. In light of the foregoing considerations, it is possible that these transitions have properly been assigned to the $Sc^{45}(n,\gamma)Sc^{46}$ reaction; but is is also possible that these transitions may be due to sample impurities or other contaminants. In either case, the burden of properly assigning these additional transitions must remain the responsibility of the authors who observed them.

The proposed level diagram (Fig. 9), summarizes states up to an excitation energy of 1645 keV, and schematically identifies those states populated directly from the capture state by upward pointing flags on the left. The states at excitation energies of 289, 627, 1088, and 1273 keV, which Van Assche *et al.*[2] had previously inferred from energy sums of the observed low-energy transitions, have been corroborated and more definitely established in the present work from the energies of the primary $\gamma$ rays alone. When the low-energy singles results (Table II) and the summaries of the coincidence studies (Tables III and IV) are combined with the results of the primary high-energy $\gamma$-ray investigation, the detailed interrelationships serve to place additional states and intervening low-energy transitions in the proposed level scheme.

As expected, primary $\gamma$-ray transitions (predominantly dipole in character) are not seen to terminate at all levels reported from the $(d,p)$ investigations. However, in several instances in which dipole transitions are allowed, the $\gamma$-ray resolution is sufficiently improved over the charged-particle resolution to resolve some states seen as single in $(d,p)$ work into close-lying doublets. It should be pointed out that below 1650 keV every state reported in the $(d,p)$ stripping studies appears to be seen also in the present $(n,\gamma)$ spectra. However, some questions of identification arise as a result of small but possibly significant energy mismatches and the fact that some states appear to be single in the $(d,p)$ spectra but are seen to be doublets in the $(n,\gamma)$. In addition, the present studies have also defined some states in this region that were not observed in the $(d,p)$ work. This confirms the introductory expectation that the combination of primary and secondary $\gamma$-ray transitions following thermal-neutron capture—which is unencumbered by the same type of selection and intensity rules that govern $(d,p)$ studies—could populate low-lying states independent of their constitution.

The 52-keV transition, between the first excited state and the ground state, was observed in the singles spectrum but was not found in any coincidence spectrum. These findings justify both its placement and isomeric nature. The results of Van Assche *et al.*,[2] Neill *et al.*,[11] and Andreeff *et al.*[6] had already dictated this placement for the 52-keV transition ($t_{1/2}=11$ $\mu$sec) in the level scheme.

The 19-sec isomeric second excited state was observed to decay by the emission of the 142-keV $\gamma$ ray in a "beam-off" experiment. The observation of a weak 8624-keV transition established the placement of this state, and the totally negative results of coincidence studies in the "beam-off" condition, immediately following "beam-on" irradiations, confirms it decay solely to the ground state. These results are in agreement with the findings of previous investigators.[2,3,11]

At this point, it may be illuminating to discuss the "227- and 228-keV" transitions which were unresolved in the present work. This low-energy "peak" was not found to be in self-coincidence. However, the coincidence spectra that involve this peak show unambiguously that it is composed of two closely spaced transitions. This peak is in coincidence with the 554- and 8539-keV $\gamma$ rays, the latter of which establishes a state at 227 keV which decays directly to the ground state. A combination of the 228-554- and 7930-554-keV coincident cascades can only be explained by the existence of a state at 280 keV, from which a strong 228-keV transition proceeds to the 52-keV isomeric first excited state. If there were only one "227-keV transition," the coincidences between this $\gamma$ ray and the 554-keV transition would imply a prompt, unobserved, and fairly strong intervening 53-keV transition. Since this "missing" transition must be either $E1$ or $M1$ (the only multipolarities with single-particle speeds fast enough to register within the 50-nsec resolving time employed), less than 25% of the decays would be expected to proceed by internal conversion. Thus the $\gamma$-ray intensity should be ample for easy observation in the coincidence studies. No evidence for a 53-keV transition was found in any coincidence spectrum. Thus, the conclusion that the "227-keV peak" is double is unavoidable. This doublet is also evident in the bent-crystal-spectrometer work of Van Assche *et al.*[2] and Neill *et al.*[11] However, it is of interest that the presence of the doublet and the placement of both the 227- and 228-keV transitions could be demonstrated in the coincidence studies without recourse to the excellent bent-crystal-spectrometer work in which this doublet was resolved.

The present coincidence studies have established the decay scheme up to the state at 1125-keV excitation energy. The only exception was the level at 774 keV, which was observed in the $(d,p)$ work of Rapaport *et al.*[1] and for which both the present work and that with the bent-crystal spectrometer[2] obtained excellent energy balances for decay by emission of a 774-keV $\gamma$ ray to the ground state and a 722-keV $\gamma$ to the 52-keV level. Except for the isomeric levels, all other states up to 1125 keV were observed to be populated and/or depopulated, as shown in the scheme of Fig. 9, in the

coincidence investigations. Several significant differences exist between the present level scheme and that proposed by Van Assche *et al.*[2] The 486-keV transition, not placed in their scheme, was seen in coincidence with the 228-keV and 554-keV transitions. These coincidence results coupled with the strength of this line strongly suggest that it is fed from the state at 1324 keV. The previous authors inferred from their accurate energies and the scintillation studies of Bolotin,[3] who reported that a peak at ~530 keV was in coincidence with the peak at ~225 keV, that the 539-keV $\gamma$ ray fed the 444-keV level. However, the present work definitely shows that this level is fed by the 547-keV $\gamma$ ray (not placed in the previous scheme), thus removing their proposed 984-keV state and supplanting it with one at 991 keV. The present work also established the 539-585-, 539-295-, and 539-7641-keV coincident cascades, thus placing the 539- keV $\gamma$ ray as proceeding from the 1125-keV level.

Several of the transitions observed in the singles $\gamma$-ray spectrum were too weak to be seen in the coincidence studies. A few of these $\gamma$ rays have been included in the decay scheme of Fig. 9 on the basis of energy balances and intensity considerations. However, it should be pointed out that although these placements are the same as those proposed by Van Assche *et al.*,[2] they are not as confidently assigned as are those inferred from the $\gamma$-ray coincidence results. Additional weak transitions, some of which were not observed in the present investigation, were placed between particular pairs of these levels by Van Assche *et al.*[2] on the basis of excellent energy balances, but are not shown on the present scheme (Fig. 9). Their absence in this scheme in no way implies that these assignments by Van Assche *et al.*[2] are not correct—it merely reflects the fact that Fig. 9 includes only those particulars of the scheme that were either established or corroborated in the present work.

Those states previously reported to be populated in the $(d,p)$ investigations[1] are shown in Fig. 9 and designated by downward pointing flags on the right. In all cases in which the energy agreement was not good enough to establish the correspondence between $(n,\gamma)$ and $(d,p)$ levels, both excitation energies are presented.

## V. DISCUSSION

### 1. Ground State

The measured[24] spin of 4, the strong $(d,p)$ population and $l_n=3$ assignment (so $\pi=+$), the primary transition to the ground state from the $3^-$ and/or $4^-$ neutron-capture state, and the characteristics[25] of the $\beta$ decay of this level to states in $Ti^{46}$, all combine to confidently assign the spin and parity of the ground state of $Sc^{46}$ as $4^+$.

### 2. 52-keV State

The 52-keV state decays directly to the $4^+$ ground state with a measured[6] half-life of $10.6\pm0.6$ $\mu$sec, which is consistent with the single-particle speed of an $E2$ transition. The strength of the $(d,p)$ population of this level is approximately twice that of any other $l_n=3$ states. Since this stripping strength is proportional to $(2J+1)$, a spin of $6^+$ is indicated. The lack of primary $\gamma$-ray population ($M2$ in this case) also is consistent with a $6^+$ assignment.

### 3. 142-keV State

The 142-keV level decays solely to the $4^+$ ground state with a half-life of 19 sec (consistent with the single-particle speed of an $E3$ or $M3$ transition). The $Ti^{47}(d,He^3)Sc^{46}$ reaction studies[4] indicate that this state has $l_p=2$ (or 0) character and therefore negative parity. The proton-hole nature of this level is consistent with its lack[1] of $(d,p)$ population. The above considerations rule out the possibility of an $M3$ assignment for the 142-keV transition and serve to limit the spin and parity of this level to either $1^-$ or $7^-$. The lack of decay from this state to the $6^+$ 52-keV level strongly favors the $1^-$ assignment. In addition, the small (but definite) primary $\gamma$-ray population from the spin $3^-$ and/or $4^-$ neutron-capture state suggests that a $1^-$ assignment for the 142-keV level (in which case the primary transition is $E2$) is to be preferred to a $7^-$ assignment (with an $E3$ primary transition).

### 4. 227-keV State

The $l_n=3$ assignment for the 227-keV state dictates a positive parity. This level decays only to the $4^+$ ground state and not to the $1^-$ 142-keV or $6^+$ 52-keV levels. This suggests a $3^+$ or $4^+$ assignment for this level and an $M1$ character for the 227-keV $\gamma$-ray transition. Primary $\gamma$-ray population of this state supports these two spin possibilities. Consideration of the decay characteristics of the 280-, 289-, 444-, and 774-keV levels proscribes the $4^+$ alternative.

### 5. 280-keV State

The proton angular distribution observed in the $(d,p)$ studies of the 280-keV state suggests an $l_n=1$ assignment and therefore a positive parity. The strong $\gamma$-ray decay of this level to the 52-keV state ($6^+$), along with the weak transition to the $4^+$ ground state, suggests a $5^+$ spin and parity assignment. The absence of a primary $\gamma$-ray transition to this level does not argue against such an assignment, despite the lack of the possible $E1$ transition to it. Since the capture state is compound statistical, the strength of transitions from unbound resonance-capture states to a given final state

[24] F. Russell Petersen and H. A. Shugart, Phys. Rev. **128**, 1740 (1962).

[25] *Nuclear Data Sheets*, compiled by K. Way *et al.* (U. S. Government Printing Office, National Academy of Sciences—National Research Council, Washington 25, D. C., 1961), NRC 60-2-30 and NRC 60-2-33.

is expected to be governed by a broad distribution of partial $\gamma$-ray widths.[26] This distribution predicts a preponderance of partial radiative transition widths that are small compared to the average radiation width for primary transitions to that final state from many resonances. The thermal-capture state (which is characterized by the weighted contribution of several resonances) may indeed have a $4^-$ contribution, but the possible $E1$ primary transition from this state to the 280-keV level ($5^+$) may be too weak to have been observed in the present work. (In this context, while a relatively strong primary transition to a given final state can be viewed as positive evidence of its low multipolarity, the lack of observation of a primary transition to a particular low-lying level does not positively rule out the possibility that a low-multipolarity transition may be allowed but be so weak as to escape detection.) From the indicated $5^+$ assignment of the 280-keV level, one might perhaps speculate that the possible $4^-$ spin contribution to the thermal-capture state is small, and the remaining $3^-$ component would raise the multipolarity of the "missing" primary transition to the 280-keV $5^+$ state to $M2$. An $M2$ transition is not expected to compete favorably with dipole primary transitions to nearby low-lying excited states. As attractive as this simplifying suggestion might appear, the statistical distribution of partial radiation widths which governs the decay of the capture state will not permit such a positive assessment to stand in the absence of additional corroborative evidence.

The lack of a 53-keV $\gamma$-ray transition from the 280-keV level to the 227-keV state has been remarked upon earlier (Sec. IV). The absence of this 53-keV transition (single-particle speed $\sim 10^{-10}$ sec for an $M1$ transition, $\sim 10^{-5}$ sec for an $E2$) in competition with the 228-keV $M1$ transition (single-particle speed $\sim 10^{-12}$ sec) to the 52-keV $6^+$ state, is consistent with both a spin and parity of $5^+$ for the 280-keV level and the $3^+$ assignment of the 227-keV state. The 280-keV ground-state transition from this level tends to exclude spins greater than $5^+$, while a $4^+$ assignment to either or both of these levels appears to be at variance with the available experimental evidence.

### 6. 289-keV State

The lack of $(d,p)$ population of this 289-keV level coupled with the proton-hole (probably $d_{3/2}^{-1}$) assignment resulting from the $(d,\mathrm{He}^3)$ studies[4] argues for a negative parity. In the present work, this level has been observed to decay to the $1^-$ isomeric state at 142-keV and to the 227-keV level via a very weak 62-keV transition in the scheme of Van Assche *et al.*[2] The prompt nature of the decay of the 289-keV state by way of the 147-keV transition, established in the present investigation, would argue against an $E2$ character for this $\gamma$ ray (single-particle speed $\sim 10^{-6}$ sec) and would tend to specify this as an $M1$ transition and restrict the spin possibilities of this level to be $\leqslant 2$. The reported assignment[2] of a 62-keV $\gamma$-ray branch from this state to the 227-keV level (preferred spin $3^+$) would suggest the assignment of some $E1$ component to this transition (single-particle speed $\sim 3\times 10^{-12}$ sec if $E1$; $\sim 10^{-3}$ sec if $M2$), in order to allow competition with the 147-keV $M1$ branch. A spin of $\leqslant 2^-$ for the 289-keV level not only discriminates against a possible $4^+$ assignment for the 227-keV state and leaves open only the $3^+$ assignment for that level, but prescribes a $2^-$ designation for the 289-keV level. The presence of a primary transition to the 289-keV level in consistent with a $2^-$ assignment (in which case the primary transition would be $M1$). The decay of the 585-keV state to this level (Sec. V8) also favors this spin assignment.

### 7. 444-keV State

The $l_n=3$ assignment for this 444-keV level, the strong decay of this level to the $3^+$ 227-keV state, and the relatively intense primary $\gamma$-ray transition populating the state under consideration leads to spin possibilities of $2^+$, $3^+$, or $4^+$ for this state. The lack of a transition between this level and the $4^+$ ground state (by way of an energy-favored $M1$ transition) suggests the exclusion of the $3^+$ and $4^+$ possibilities, and leaves the $2^+$ assignment for this level. If the placement of an extremely weak 302-keV $\gamma$-ray branch from this state to that at 142-keV ($1^-$) (which Van Assche *et al.*[2] hesitantly proposed) is correct, the $2^+$ assignment of the 444-keV level is somewhat strengthened.

### 8. 585-keV State

The lack of significant $(d,p)$ population[2] and the proton-hole character[4] (probably $l_p=2$) for this 585-keV state, are mutually consistent and specify negative parity. The 8182-keV primary transition to this level is by far the most intense seen to any of the low-lying states. The parities of the initial and final states require an $M1$ transition and restrict the spin possibilities of the 585-keV level to be $2^-$, $3^-$, $4^-$, or $5^-$. The strong decay of this state to both the 289-keV ($2^-$) state and ground state ($4^+$) favors a $3^-$ assignment. The weak branching to the 227-keV ($3^+$) and 142-keV ($1^-$) levels assigned by Van Assche *et al.*[2] supports this $3^-$ designation.

### 9. 627-keV State

The absence of observed $(d,p)$ strength[2] to this 627-keV level, and the probable $l_p=2$ or 0 proton-hole nature[4] of this state label it as negative parity. The strong 627-keV transition from this level to the ground state ($4^+$), the weak 400-keV $\gamma$-ray branch to the 227-keV $3^+$ level, and the lack of branching to any other lower-lying state (especially to the $2^-$ proton-hole state at 289-keV) help to establish this as a $4^-$ level. The

[26] C. E. Porter and R. G. Thomas, Phys. Rev. **104**, 483 (1956).

primary $\gamma$-ray transition to this state is consistent with this assignment.

### *10. 774-keV State*

The $l_n=1$ or 3 (therefore positive parity) assignment to the 774-keV state and the decay of this level to the spin-$4^+$ ground state and $6^+$ first excited state suggests an assignment of $5^+$ for this level. The absence of a branch to the 227-keV state is also consistent with the $3^+$ assignment of that level.

### *11. 835-keV State*

The observed decay of the 835-keV level to the $5^+$ state at 280 keV and to the $4^+$ ground state and also the lack of an observed branch $\gamma$ ray to the 227-keV $3^+$ excited state point to spin 5 for this state—although the lack of a transition to the $6^+$ first excited state is not explained. The $l_n=1$ or 3 assignment for the 835-keV level specifies positive parity. The 7930-keV primary transition to this level is not inconsistent with this spin assignment.

### *12. 991-keV State*

The 547-keV transition from the 991-keV state to the $2^+$ level at 444 keV and the lack of observed branching to any other low-lying state of positive parity makes a $1^+$ assignment attractive for the 991-keV state. The absence of primary population of this level ($M2$, in this case) is consistent with this possible spin and parity. The lack of possible $E1$ transitions to the 147-keV ($1^-$) and 289-keV ($2^-$) states would argue against a $1^+$ assignment, but shell-model considerations (see below) would tend to soften this objection.

### *13. 1088-keV State*

The branching of this state to the 227-keV ($3^+$) and 280-keV ($5^+$) levels supports a $4^+$ assignment for the 1088-keV level. The $l_n=1$ $(d,p)$ assignment[1] fixes the parity as positive. The presence of a 7675-keV primary transition to this state is consistent with this $4^+$ assignment.

### *14. Higher Excited States*

Although several transitions are shown as proceeding from the 1125-keV state, their placements are not certain enough (except for the 539-keV transition) to allow a meaningful discussion of the decay of this level. Similarly, the lack of definitive evidence about the decay of higher excited states to lower-lying levels precludes any detailed assessments of the possible spins and parities of these levels.

Considerations of regional shell-model systematics lead to the expectation that the low-lying positive-parity states would be dominated by the $\pi(f_{7/2})\nu(f_{7/2})^5$ configuration ($\pi$=protons, $\nu$=neutrons) and that the negative-parity levels would be characterized primarily by $d_{3/2}$ and/or $s_{1/2}$ proton-hole configurations. The levels which have been most confidently assigned negative parity are those at 142, 289, 585, and 627 keV. In the $(d,\mathrm{He}^3)$ work of Yntema *et al.*,[4] these states show strong indications of $l_p=2$ ($d_{3/2}$ proton-hole) character. With the possible exception of the 280-keV level (probably $l_n=1$), all of the low-lying positive-parity states have been assigned $l_n=3$ and, in general, are consistent with the $\pi(f_{7/2})\nu(f_{7/2})^5$ configuration prescribed by the calculations of McCullen *et al.*[11] Thus, the available evidence indicates that these anticipated configurations will be dominant in the low-lying states of $Sc^{46}$.

These particular configurations would permit $M1$ transitions between states of like parity, while $E1$ transitions would be forbidden between states of different parity. Indeed, the presence of only these configurations would imply transitions with $M2$ or higher multipolarity between states of dissimilar parentage.

The observed successful competition of transitions from several initial negative-parity levels to lower-lying states of both parities can be taken as evidence of the presence of anticipated admixtures of other configurations; if only these pure configurations were involved, an abnormally large $M1$ retardation factor of $\sim 10^5$ would necessarily be implied. The invocation of some configuration admixtures conducive to $E1$ radiation appears to be required in order that transitions between states of unlike parity can proceed with speeds comparable to competing $M1$ transitions that feed final states of like parity. The magnitude of such admixtures is difficult to assess from the available experimental evidence without certain simplifying assumptions. The known $M2$ and $E1$ retardations observed in this mass region[27] preclude any detailed evaluation of these admixtures on the basis of estimates of the single-particle speeds of the transitions involved. However, calculations based upon the questionable application of single-particle estimates point to the need of less than $\sim 0.1\%$ admixtures of $E1$-conducive configurations to account for the observed decay characteristics of the low-lying states of $Sc^{46}$. One can conceive of several such configuration components; but in the absence of the additional information needed to decide among them, even their enumeration is pointless.

## VI. EXPERIMENTAL ASIDE

At this point it might be appropriate to compare the techniques exploited in the present work with those previously empolyed in the study of the low-lying excited states of $Sc^{46}$. Any generalizations based upon such a comparison are equally valid for a host of similar neutron-capture $\gamma$-ray studies.

Firstly, $(d,p)$, $(d,\mathrm{He}^3)$, and other charged-particle reactions can provide a great deal of information con-

[27] D. Kurath and R. D. Lawson, Phys. Rev. **161**, 915 (1967).

cerning the detailed parameters of levels populated (e.g., the excitation energy, orbital angular momentum, spin in certain favorable cases, etc.) and can help to establish the particle or hole character of these states. The combination of these data with that of neutron-capture $\gamma$-ray studies, not only adds information concerning those states not populated in any particular one of these types of investigations, but also can provide salient details of the properties of states seen in both studies. These details include $\gamma$-ray branching ratios, limitations on (or determination of) spin and parity, insight into configuration mixing, and the like.

Secondly, and of more experimental import, is the comparison of the present methods with other $(n,\gamma)$ techniques. Certainly, the high-resolution Ge(Li) singles spectroscopic studies of primary transitions that populate low-lying excited states are recognized as the most definitive of all techniques empolyed to study the spectra of these transitions. These investigations provide several types of important information, the simplest and most straightforward being the establishment of accurate excitation energies for a host of low-lying excited states. What is more to the point, however, is the type of information that can be obtained about transitions between these low-lying excited states, the delineation of additional states of low excitation energy not populated in charged-particle or primary $\gamma$-ray studies, and the determination of the $\gamma$-ray branching to and from the latter states. The greatly superior energy resolution of bent-crystal spectrometers below $\gamma$-ray energies of $\sim$2 MeV is capable of providing information about more, and weaker, low-energy transitions than is the Ge(Li) detector. However, the establishment of a coherent level scheme from bent-crystal-spectrometer data, even in combination with information gleaned from charged-particle and primary $(n,\gamma)$ transitions, depends upon precise energy balances. Unfortunately, a level scheme based on this technique is, to some extent, dependent upon confidence that the statistical expectation for accidental energy balances is extremely small. However, since the $(n,\gamma)$ process populates a myraid of low-lying states, there are often several pairs of levels between which a given transition might be placed. Thus, the comfort provided by small accidental energy balance probabilities does not engender the highest degree of soul-satisfying reliance, despite overwhelming appreciation for the degree of accuracy associated with these energy sums.

On the other hand, although not blessed with the energy resolution necessary to resolve all of the transitions observable by bent-crystal spectroscopy, Ge(Li) detectors can be empolyed in singles and $\gamma$-$\gamma$ coincidence studies between low-energy transitions and both high-energy primary transitions and low-energy transitions. In such applications, they are not only capable of revealing many or most of these transitions that are not of the weakest intensity, but can also establish unequivocal data concerning the sequential ordering of these transitions, and thus a more positive determination of much of the level scheme. As an almost trival example in the case of $Sc^{46}$, it is the opinion of this author that the established coincidence relationship between the 8539-keV primary transition and the 227-keV $\gamma$ ray provides more convincing evidence of the placement of the latter transition than does the fact that their energies sum to the binding energy. The coincidence between them demands that the cascade proceed to the ground state; a precise energy sum can only establish a high probability that they do, since it is extremely difficult for the energy sum to unequivocally reject the possible placement of the 227-keV $\gamma$ ray elsewhere in the scheme.

These declamatory comparisons are not without their compromising grace, for it seems obvious that it is only the combined information gleaned from the use of both techniques that can provide the most comprehensive and complete establishment of the level scheme. Fortunately, most shortcomings of one method are compensated by the strengths of the other. Neither alone may be totally adequate in the general case, although either by itself may provide sufficiently complete and accurate information in specific studies.

## ACKNOWLEDGMENTS

The author wishes to express his appreciation to M. G. Strauss and co-workers for the design and construction of the two-parameter magnetic-tape analyzer and high-counting-rate electronics, to H. Mann and co-workers, who provided the Ge(Li) detectors and preamplifiers, to G. E. Thomas, who designed the through-hole facility and installed the samples, to D. W. Engelkemeir, who supplied the calibrated sources, to C. E. Batson, who recorded and processed much of the data, and to D. A. McClure, for his aid in some portions of the analysis.